On the triplet distribution and its effect on an improved phosphorescent organic light-emitting diode

S. W. Liu, Y. Divayana, A. P. Abiyasa, S. T. Tan, H. V. Demir, and X. W. Sun

Articles you may be interested in

Highly efficient greenish-blue platinum-based phosphorescent organic light-emitting diodes on a high triplet energy platform
Appl. Phys. Lett. **104**, 173303 (2014); 10.1063/1.4875240

Distinguishing triplet energy transfer and trap-assisted recombination in multi-color organic light-emitting diode with an ultrathin phosphorescent emissive layer
J. Appl. Phys. **115**, 114504 (2014); 10.1063/1.4869056

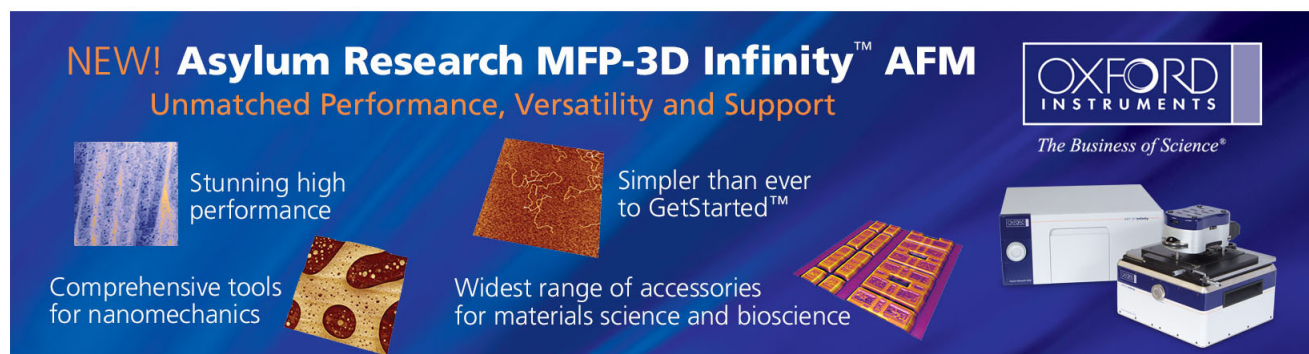Effects of mixed host spatial distribution on the efficiency of blue phosphorescent organic light-emitting diodes
Appl. Phys. Lett. **101**, 043303 (2012); 10.1063/1.4739499

Improved performance of blue phosphorescent organic light-emitting diodes with a mixed host system
Appl. Phys. Lett. **95**, 253304 (2009); 10.1063/1.3276075

Efficiency improvement of phosphorescent organic light-emitting diodes using semitransparent Ag as anode
Appl. Phys. Lett. **88**, 033509 (2006); 10.1063/1.2164901

On the triplet distribution and its effect on an improved phosphorescent organic light-emitting diode

S. W. Liu,[1] Y. Divayana,[1,2] A. P. Abiyasa,[1] S. T. Tan,[1] H. V. Demir,[1,3,4,a)] and X. W. Sun[1,5,b)]

[1]*Luminous! Center of Excellence for Semiconductor Lighting and Displays, School of Electrical and Electronic Engineering, Nanyang Technological University, Nanyang Avenue, Singapore 639798*
[2]*School of Electrical Engineering, Udayana University, Kampus Bukit Jimbaran, Bali, Indonesia*
[3]*School of Physical and Mathematical Sciences, Nanyang Technological University, Nanyang Avenue, Singapore 639798*
[4]*Department of Electrical and Electronics Engineering and Department of Physics, UNAM-National Nanotechnology Research Center, Bilkent University, Bilkent, Ankara 06800, Turkey*
[5]*Department of Applied Physics, College of Science, and Tianjin Key Laboratory of Low-Dimensional Functional Material Physics and Fabrication Technology, Tianjin University, Tianjin 300072, China*

We reported phosphorescent organic light-emitting diodes with internal quantum efficiency near 100% with significantly reduced efficiency roll-off. It was found that the use of different hole transporting layer (HTL) affects the exciton distribution in the emission region significantly. Our best device reaches external quantum efficiency (EQE), current, and power efficiency of $22.8\% \pm 0.1\%$, 78.6 ± 0.2 cd/A, 85 ± 2 lm/W, respectively, with half current of 158.2 mA/cm^2. This considerably outperforms the control device with N,N$'$-bis(naphthalen-1-yl)-N,N$'$-bis(phenyl)-benzidine (NPB) (HTL) and 4,4$'$-N,N$'$-dicarbazole-biphenyl (host) with maximum EQE, current and power efficiency of $19.1\% \pm 0.1\%$, 65.6 ± 0.3 cd/A, 67 ± 2 lm/W, respectively, with half current of only 8.1 mA/cm^2. © *2012 American Institute of Physics*. [http://dx.doi.org/10.1063/1.4749278]

Organic light-emitting diodes (OLEDs) have been regarded as the next generation display and lighting technologies because of their potential to achieve high efficiency at low cost and flexible form factor.[1] Since the first report of phosphorescent organic light emitting diodes (PHOLEDs) using *fac* tris(2-phenyl-pyridinato-N,C$^{2'}$) iridium (Ir(ppy)$_3$) as phosphorescent dye,[2] continuous efforts have been made to improve the external quantum efficiency (EQE) from an initial value of 8% to more than 20% recently.[1–5]

N,N$'$-bis(naphthalen-1-yl)-N,N$'$-bis(phenyl)-benzidine (NPB) has been extensively used as hole transporting layer (HTL), further studies on OLEDs with NPB used as HTL and 4,4$'$-N,N$'$-dicarbazole-biphenyl (CBP): Ir(ppy)$_3$ as an emission layer (EML) showed that the recombination zone was close to the HTL/EML interface.[6,7] However, such OLEDs were inefficient because of the lower triplet energy of NPB (2.3 eV) as compared to that of Ir(ppy)$_3$ (2.4 eV).[8,9] Therefore, material with higher triplet energy had to be used at the EML interface to confine the excitons within the EML.

Recently 4,4$'$,4$''$-tris(N-carbazolyl)triphenylamine (TCTA) has been used as HTL owing to its excellent hole mobility of around 10^{-4} cm^2/V/s and high triplet energy of 2.7 eV.[10,11] However, TCTA is not an ideal candidate for host layer due to its poor electron transport capability.[11] CBP on the other hand has ambipolar charge transporting capability with both hole and electron mobilities around 10^{-4} cm^2/V/s at an applied field of 0.5 MV/cm.[11] Moreover, the HOMO level of 6.1 eV and LUMO of 2.8 eV of CBP are almost ideal for host with relatively wide bandgap.

In this paper, we use TCTA as the hole transporting layer and CBP as the host layer. Significant improvement

was achieved compared to the control device that uses NPB as HTL. The EQE of the best device reaches $22.8\% \pm 0.1\%$ with a maximum power efficiency of 85 ± 2 lm/W. The EQE roll-off was also significantly improved with TCTA as the HTL. At high current density of 22 mA/cm^2, the best EQE is almost doubled compared to the control device. To our knowledge, this is one of the highest reported EQEs for CBP host without external light out-coupling. We found that the triplet exciton distribution is significantly altered and the half current is improved by almost 20 times with the usage of TCTA compared to the control device with NPB as HTL. The improvement in the device performance results from better exciton distribution and confinement in the emission layer.[12,13] The details of the device fabrication and measurement can be found elsewhere.[14,15]

Devices with the following configurations were fabricated: **S1**, ITO/MoO$_3$ (10 nm)/NPB (60 nm)/CBP: Ir(ppy)$_3$ (5%, 20 nm)/Bphen (50 nm)/LiF (1 nm)/Al (100 nm); **S2**, ITO/MoO$_3$ (10 nm)/NPB (40 nm)/TCTA (20 nm)/CBP: Ir(ppy)$_3$ (5%, 20 nm)/Bphen (50 nm)/LiF (1 nm)/Al (100 nm); and **S3**, ITO/MoO$_3$ (10 nm)/TCTA (60 nm)/CBP: Ir(ppy)$_3$ (5%, 20 nm)/Bphen (50 nm)/LiF (1 nm)/Al (100 nm). For all three devices, MoO$_3$ is used as the hole injection layer (HIL), CBP: Ir(ppy)$_3$ is the EML, 4,7-diphenyl-1,10-phenanthroline (Bphen) is the electron transport layer (ETL) and hole blocking layer (HBL), LiF is the electron injection layer (EIL), and Al is the cathode. The only difference among them is the choice of HTL, for the control device S1, NPB is used as HTL, while S2 uses NPB and TCTA as HTL, in device S3, TCTA serves as HTL. Figure 1 shows the structure and band diagram of various devices investigated in this work, the energy levels are extracted from literatures.[4,16,17]

Figure 2 shows the current density versus voltage (J-V) and luminance versus current density (L-J) curves for various

a)Electronic mail: volkan@stanfordalumni.org.
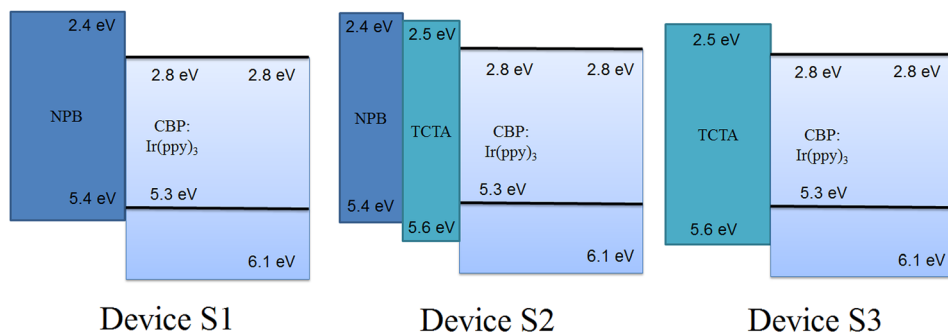b)Electronic mail: exwsun@ntu.edu.sg.

FIG. 1. Device structure and energy bands for S1, S2, and S3.

devices shown in Figure 1. From Figure 2(a), it can be seen that all devices exhibit similar J-V characteristics, despite of the variation of the hole energy barrier and mobility, e.g., HOMO values of NPB and TCTA are 5.4 eV and 5.6 eV, respectively,[18] and NPB has a slight larger hole mobility of 4×10^{-4} cm^2/V/s as compared to TCTA (1×10^{-4} cm^2/V/s).[8,10] The L-J curves on the other hand significantly differ for all devices. Figure 2(b) shows that S3 has much larger luminance, which implies improved recombination efficiency as compared to S1 and S2. At a low current density of 0.01 mA/cm^2, the operating voltage of devices S1, S2, and S3 are 3.0 V, 3.1 V, and 3.0 V, at a brightness level of 6.5 ± 0.2 cd/m^2, 6.4 ± 0.1 cd/m^2, and 7.9 ± 0.1 cd/m^2, respectively. The brightness reaches 6578 ± 74 cd/m^2, 9870 ± 110 cd/m^2, and 14245 ± 77 cd/m^2, respectively, at the same current density of 22.2 mA/cm^2.

Figure 3 shows the EQE, current, and power efficiency versus current density for devices S1, S2, and S3. Compared to the control device S1, which has maximum power efficiency (current efficiency) of 67 ± 2 lm/W (65.6 ± 0.3 cd/A), S2 shows a similar performance with power efficiency (current efficiency) of 66 ± 1 lm/W (63.7 ± 0.6 cd/A), while S3 has improved performance with maximum power efficiency (current efficiency) of 85 ± 2 lm/W (78.6 ± 0.2 cd/A). Furthermore, the control device S1 shows significant efficiency roll-off, for example, the efficiency drops from 61.0 ± 0.1 cd/A (56.0 ± 0.3 lm/W) to 34.1 ± 0.4 cd/A (18.2 ± 0.3 lm/W) when the current density changes from 0.1 mA/cm^2 to 10 mA/cm^2. For comparison, much reduced efficiency roll-off happens for device S3 from 77.5 ± 0.2 cd/A (68.7 ± 0.7 lm/W) to 69.5 ± 0.1 cd/A (35.4 ± 0.1 lm/W), for the same current range. Similarly, device S2 also has a better roll-off compared to S1 where it drops from 61 ± 1 cd/

A (54 ± 1 lm/W) to 49.0 ± 0.4 cd/A (24.6 ± 0.3 lm/W). The control device S1 has a peak EQE of only $19.1 \pm 0.1\%$, while S2 and S3 reach higher EQE of $19.9\% \pm 0.1\%$ and $22.8\% \pm 0.1\%$, respectively. The EQE roll-off of S2 and S3 has also improved significantly compared to S1. To ensure device S1 is optimized, we fabricated devices with different NPB thickness, ITO/MoO$_3$ (10 nm)/NPB (X nm)/CBP: Ir(ppy)$_3$ (5%, 20 nm)/Bphen (50 nm)/LiF (1 nm)/Al (100 nm), where X is set to 40, 50, 60, and 70 nm, respectively. The inset of Figure 3(b) shows the maximum EQE of the device as a function of the NPB thickness. The device S1 with a NPB layer of 60 nm shows the best performance, and hence it is used as the control device.

To better understand the factors causing such significant improvement, we study the triplet exciton distribution for each device. To do so, we fabricated the following structures: **E1**, ITO/MoO$_3$ (10 nm)/NPB (60 nm)/CBP (X nm)/CBP: Ir(ppy)$_3$ (5%, 5 nm)/CBP (15−X nm)/Bphen (50 nm)/LiF (1 nm)/Al (100 nm), **E2**, ITO/MoO$_3$ (10 nm)/NPB (40 nm)/TCTA (20 nm)/CBP (X nm)/CBP: Ir(ppy)$_3$ (5%, 5 nm)/CBP (15−X nm)/Bphen (50 nm)/LiF (1 nm)/Al (100 nm), and **E3**, ITO/MoO$_3$ (10 nm)/TCTA (60 nm)/CBP (X nm)/CBP: Ir(ppy)$_3$ (5%, 5 nm)/CBP (15−X nm)/Bphen (50 nm)/LiF (1 nm)/Al (100 nm). The 5 nm CBP: Ir(ppy)$_3$ EML acted as a sensing layer, by varying the value of X from 0 to 5 nm, 10 nm, and 15 nm, respectively, the average exciton distribution profile within the 20 nm thick CBP host layer can be revealed.

Inset of Figure 4(a) shows the average triplet exciton distribution profile (normalized EQE) within the host layer. It can be seen that triplet exciton distributions are significantly different for device E1, E2, and E3. The normalized EQE is fitted using the following diffusion equation:[19]
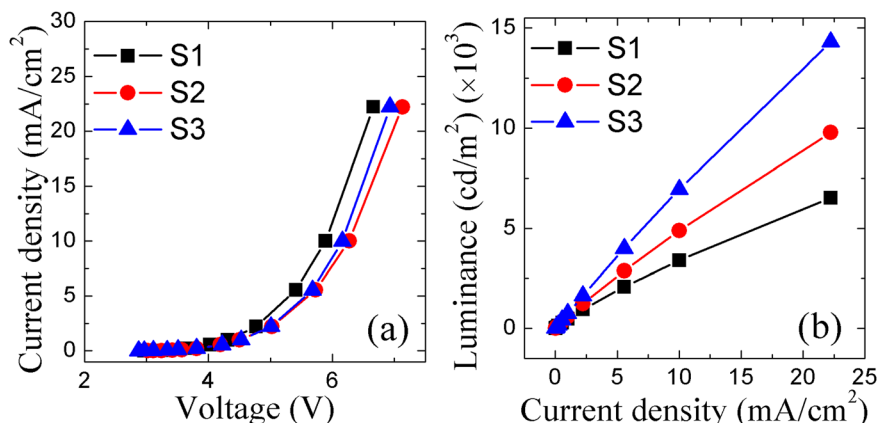

FIG. 2. (a) Current density versus voltage (J-V) and (b) luminance versus current density (L-J) for devices S1, S2, and S3.
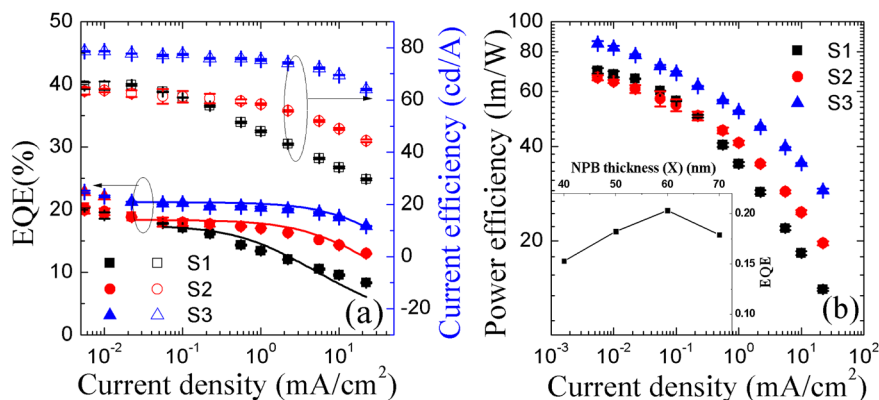
FIG. 3. (a) EQE with fitting and current efficiency versus current density and (b) power efficiency versus current density for devices S1, S2, and S3. Inset of (b) shows the maximum EQE as a function of the NPB thickness (X).

$$y = Ae^{-\frac{x}{L_D}} + Be^{\frac{x-d}{L_D}}, \qquad (1)$$

where A and B represent for the relative peak triplet exciton concentration at the CBP/HTL and CBP/Bphen interfaces, L_D is the diffusion length of triplet in CBP, and d is the thickness of EML. In our case, $d = 20$ nm. By fitting, we obtained the diffusion length L_D to be around 14 nm. The value of excion diffusion length obtained here is smaller than 46 nm reported in the literature.[19] This is perhaps due to the thin EML, where Forster resonance energy transfer (FRET) and Dexter energy transfer between host and guest still dominate the exciton distribution instead of direct exciton diffusion. A and B are 0.8 and 0.4 for E1, 0.3 and 1.1 for E2, 0.4 and 1.2 for E3, respectively. The larger A value in E1 indicates the peak exciton concentration is located at CBP/NPB interface, while the larger B values for E2 and E3 means the peak exciton concentration shifts to CBP/Bphen interface.

Figure 4(a) [(i)–(iii)] depicts the emission spectrum with respect to distance (X) between phosphorescent dopants sites to CBP/HTL interface for devices E1, E2, and E3 at current density of 0.22 mA/cm^2, respectively. From Figure 4(a) (i), where NPB is used as HTL, when the Ir(ppy)$_3$ doping was placed at NPB/CBP interface (X = 0), we mainly observed the emission spectrum with a peak around 510 nm. When the Ir(ppy)$_3$ doping was moved towards the cathode side, however, we observed an additional blue emission with a peak around 460 nm, which corresponds to the emission of NPB.[20] Furthermore, an increase in NPB emission is observed as the Ir(ppy)$_3$ doping was moved away from the NPB/CBP interface. We can conclude that majority of excitons are formed at the NPB/CBP interface. This is why when the sensing layer was moved away from the interface, the

blue emission is increased compared to green emission. EQE of device E1 at X = 0 is very small (only around 5%), which indicates that most of Ir(ppy)$_3$ triplet emission is quenched by the NPB. This is because triplet energy of NPB (2.3 eV)[8] is lower compared to the triplet energy of Ir(ppy)$_3$ (2.4 eV).[9]

Figure 4(a) [(ii) and (iii)] shows the emission spectrum for device E2 and E3, respectively, where TCTA was placed at HTL/CBP interface. Regardless of the position of the sensing layer, only emission from Ir(ppy)$_3$ was observed. This means that the structure provides a better exciton confinement within the emission layer. From the inset of Figure 4(a), we can clearly see that the exciton formation zone is located at CBP/Bphen interface for device E2 and E3, and E3 has a more uniform exciton distribution compared to that of E2. By relating the emission spectrum and triplet exciton distribution of E1, E2, and E3 with the performance of S1, S2, and S3, respectively, we can conclude that the more balanced exciton distribution and better confinement are the reasons why S3 performs the best.

To understand the hidden reason why S3 has a better exciton distribution over S2 and S1, we study the electrical behaviour of the hole only devices as follows: **H1**, ITO/MoO$_3$ (20 nm)/NPB (60 nm)/CBP (70 nm)/Al (100 nm), **H2**, ITO/MoO$_3$ (20 nm)/NPB (40 nm)/TCTA (20 nm)/CBP (70 nm)/Al (100 nm), and **H3**, ITO/MoO$_3$ (20 nm)/TCTA (60 nm)/CBP (70 nm)/Al (100 nm).

Figure 4(b) shows the current density of device H1, H2, and H3. We observed that H1 has the smallest current flow as compared to device H2 and H3. This is because for H1, the holes need to overcome a large energy barrier (0.7 eV) at NPB/CBP interface. For device H2, the addition of 20 nm TCTA layer introduces a step barrier that facilitates better
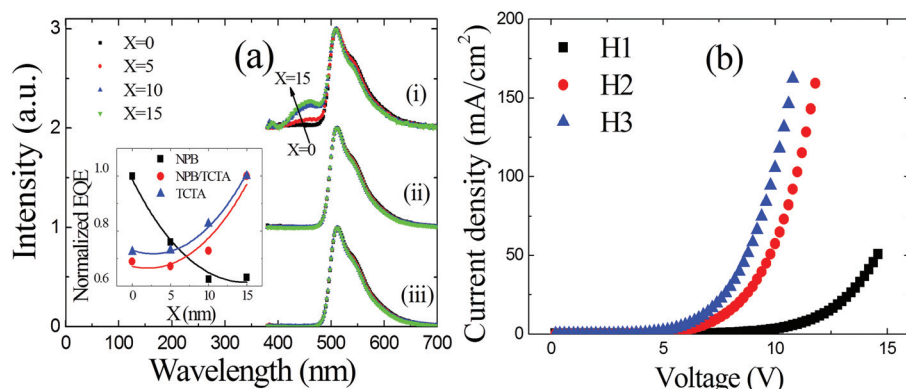

FIG. 4. (a) Emission spectrum of (i) E1, (ii) E2, and (iii) E3 at the current density of 0.22 mA/cm^2 when the sensing layer was placed at X = 0, 5 nm, 10 nm, and 15 nm. (b) J-V characteristics of hole-only devices H1, H2, and H3. Inset of (a) shows the average triplet exciton distribution profile within CBP host for devices E1, E2, and E3.

hole transport to the CBP.[21,22] Improvement in hole injection and transport towards CBP/Bphen interface shifts the exciton formation zone toward CBP/Bphen interface. The use of TCTA layer only in device H3 eliminates the hole accumulation at the NPB/TCTA interface, which further improves the hole injection into the CBP layer as compared to H2, increasing the recombination efficiency. A recent study in the literature showed that a universal energy alignment trend between transition oxide and organic semiconductors, if the Fermi level of the oxide lies below the HOMO of the organic semiconductors, the HOMO level of the organic material will be pinned at the Fermi level of the oxide,[23] this will result in efficient charge injection from oxide into organic semiconductors. Therefore, because of the much deeper lying LUMO (6.7 eV) of MoO_3 as compared to the HOMO values of NPB (5.4 eV) and TCTA (5.6 eV),[18] efficient hole injection from MoO_3 into both NPB and TCTA was anticipated.[14,15,24] The elimination of multiple interfaces and a smaller hole energy-barrier at TCTA/CBP for device S3 therefore improves the hole injection significantly.

It is known that EQE roll-off is caused mainly by triplet-triplet annihilation (TTA) at high intensity, which is due to the long lifetime of the triplet excitons.[25,26] The EQE follows[27]

$$\eta = \eta_o \frac{J_o}{4J} \left[\sqrt{1 + \frac{8J}{J_o}} - 1 \right], \qquad (2)$$

where $J_o = \frac{4dq}{k\tau^2}$, τ is the triplet lifetime (s), k is the TTA rate (cm^3/s), d is the thickness of the organic layer (nm), while q is the elementary charge. If we let $J = J_o$, Eq. (2) results in $\eta = \frac{1}{2}\eta_o$; therefore, J_o is also known as the half current density. The EQEs of all devices shown in Figure 3(a) are fitted using Eq. (2), the half current density J_o of S3 is 158.2 mA/cm^2, more than twice that of S2 (60.0 mA/cm^2) and almost 20 times larger compared to that of S1, which is only 8.1 mA/cm^2. The higher half current density means significantly reduced efficiency roll-off and better device stability. However from Eq. (2), it is clear that the half-current density is only influenced by the thickness of EML (d) and exciton's lifetime (τ). Therefore, it is expected that J_o does not vary for all devices. The possible explanation why S2 and S3 have much improved roll-off than S1 is because the formers provide better exciton confinement at higher current density. The severe EQE roll-off for S1 is caused by the leakage of exciton toward NPB at higher current due to lower triplet energy bandgap. Therefore, it is imperative to have TCTA at the interface for a better confinement. For device S3, the excitons are more evenly distributed, and TTA is thus less severe.

In conclusion, we have reported a highly efficient OLED with EQE of 22.8% ± 0.1% and power efficiency of 85 ± 2 lm/W without external out-coupling. This was achieved by employing TCTA as the HTL and CBP as host layer. With better triplet exciton distribution and confinement, the efficiency roll-off was significantly reduced with much improved half current density of 158.2 mA/cm^2.

[1]Z. B. Wang, M. G. Helander, J. Qiu, D. P. Puzzo, M. T. Greiner, Z. M. Hudson, S. Wang, Z. W. Liu, and Z. H. Lu, Nat. Photonics **5**(12), 753 (2011).
[2]M. A. Baldo, S. Lamansky, P. E. Burrows, M. E. Thompson, and S. R. Forrest, Appl. Phys. Lett. **75**(1), 4 (1999).
[3]S. O. Jeon and J. Y. Lee, Org. Electron. **12**(11), 1893 (2011).
[4]Z. B. Wang, M. G. Helander, J. Qiu, D. P. Puzzo, M. T. Greiner, Z. W. Liu, and Z. H. Lu, Appl. Phys. Lett. **98**(7), 073310 (2011).
[5]A. Haldi, B. Domercq, B. Kippelen, R. D. Hreha, J. Y. Cho, and S. R. Marder, Appl. Phys. Lett. **92**(25), 253502 (2008).
[6]H. Yamamoto, C. Adachi, M. S. Weaver, and J. J. Brown, Appl. Phys. Lett. **100**(18), 183306 (2012).
[7]J. Y. Lee, Appl. Phys. Lett. **89**(15), 153503 (2006).
[8]S. O. Jeon, K. S. Yook, C. W. Joo, J. Y. Lee, K. Y. Ko, J. Y. Park, and Y. G. Baek, Appl. Phys. Lett. **93**(6), 063306 (2008).
[9]M. A. Baldo and S. R. Forrest, Phys. Rev. B **62**(16), 10958 (2000).
[10]T. J. Park, W. S. Jeon, J. W. Choi, R. Pode, J. Jang, and J. H. Kwon, Appl. Phys. Lett. **95**(10), 103303 (2009).
[11]J. W. Kang, S. H. Lee, H. D. Park, W. I. Jeong, K. M. Yoo, Y. S. Park, and J. J. Kim, Appl. Phys. Lett. **90**(22), 223508 (2007).
[12]T. H. Zheng and W. C. H. Choy, Adv. Funct. Mater. **20**(4), 648 (2010).
[13]T. H. Zheng, W. C. H. Choy, C. L. Ho, and W. Y. Wong, Appl. Phys. Lett. **95**(13), 133304 (2009).
[14]S. W. Liu, Y. Divayana, X. W. Sun, Y. Wang, K. S. Leck, and H. V. Demir, Opt. Express **19**(5), 4513 (2011).
[15]S. W. Liu, X. W. Sun, and H. V. Demir, AIP Adv. **2**(1), 012192 (2012).
[16]C. H. Hsiao, S. W. Liu, C. T. Chen, and J. H. Lee, Org. Electron. **11**(9), 1500 (2010).
[17]W. S. Jeon, T. J. Park, S. Y. Kim, R. Pode, J. Jang, and J. H. Kwon, Appl. Phys. Lett. **93**(6), 063303 (2008).
[18]M. Kroger, S. Hamwi, J. Meyer, T. Riedl, W. Kowalsky, and A. Kahn, Appl. Phys. Lett. **95**(12), 123301 (2009).
[19]Y. R. Sun, N. C. Giebink, H. Kanno, B. W. Ma, M. E. Thompson, and S. R. Forrest, Nature **440**(7086), 908 (2006).
[20]S. H. Kim, J. Jang, and J. Y. Lee, Appl. Phys. Lett. **91**(8), 083511 (2007).
[21]F. Nuesch, M. Carrara, M. Schaer, D. B. Romero, and L. Zuppiroli, Chem. Phys. Lett. **347**, 311 (2001).
[22]W. H. Kim, A. J. Makinen, N. Nikolov, R. Shashidhar, H. Kim, and Z. H. Kafafi, Appl. Phys. Lett. **80**(20), 3844 (2002).
[23]M. T. Greiner, M. G. Helander, W. M. Tang, Z. B. Wang, J. Qiu, and Z. H. Lu, Nature Mater **11**(1), 76 (2012).
[24]Z. B. Wang, M. G. Helander, J. Qiu, Z. W. Liu, M. T. Greiner, and Z. H. Lu, J. Appl. Phys. **108**(2), 024510 (2010).
[25]S. Reineke, G. Schwartz, K. Walzer, M. Falke, and K. Leo, Appl. Phys. Lett. **94**(16), 163305 (2009).
[26]S. Reineke, K. Walzer, and K. Leo, Phys. Rev. B **75**(12), 125328 (2007).
[27]M. A. Baldo, C. Adachi, and S. R. Forrest, Phys. Rev. B **62**(16), 10967 (2000).